Predicting pyrogenic organic matter mineralization from its initial properties and implications for carbon management

Thea Whitman, Kelly Hanley, Akio Enders, Johannes Lehmann *

Department of Crop and Soil Science, Cornell University, Ithaca, NY 14853, United States

A B S T R A C T

Predicting pyrogenic carbon (PyC) or biochar stability from its precursor properties is critical for evaluating and managing terrestrial C stocks. Transmission mode Fourier transform infrared spectroscopy (FTIR) spectroscopy was compared with proximate analysis data and H/C and O/C for predicting C mineralization. PyC produced at 7 different temperatures from 6 different feedstocks, in addition to the original feedstock materials, was incubated for 3 yr at 30 °C in a sand matrix. A C debt or credit ratio was calculated by comparing the C remaining in the incubated PyC sample (accounting for the measured C lost during initial PyC production) to the C remaining in the incubated original feedstock. A value > 1 indicates that more C remains in the PyC than in the original feedstock (credit), while a value < 1 indicates a debt. After 3 yr, PyC produced at 300 °C lost significantly more C than higher temperature PyC material, but significant differences in C loss between PyC produced at temperatures $\geqslant$ 350 °C were not detectable. The best predictor of C loss was a multiple linear regression model using the fractional FTIR signals at 816, 1048, 1374, 1424, 1460, 1590, 1700 and 2925 cm^{-1} as parameters (R^2 0.80, $p < 0.0001$). After 3 yr, the C debt or credit ratio reached values significantly > 1 for all corn PyC samples and some bull, dairy and poultry PyC samples, resulting in net C credit, while all pine and oak PyC samples remained in debt. This C debt or credit ratio reveals that, depending on the timeline of interest, producing relatively low temperature PyC with less initial C loss can result in greater C savings than producing higher temperature PyC, even though the C remaining after exposure to higher pyrolysis temperatures is more stable.

© 2013 Elsevier Ltd. All rights reserved.

1. Introduction

The spectrum of material produced during incomplete combustion of biomass is heterogeneous and ranges from partially charred organic matter (OM) to charcoal, soot and graphite (Masiello, 2004; Preston and Schmidt, 2006; Krull et al., 2008). Diverse terms are used to refer to these materials, but here, we use the term pyrogenic carbon (PyC) to refer to carbon (C)-rich organic material produced by partial combustion or pyrolysis (Bird and Ascough, 2012). While PyC can be degraded both chemically and biologically, the decomposition occurs at a slow rate, with mean residence time estimated between 10^2 and 10^7 yr (Spokas, 2010; Zimmerman, 2010; Singh et al., 2012a). If this mineralization rate is slower than for fresh OM, the production of PyC could act as a C sink (Ohlson et al., 2009). The low "mineralizability" of PyC has resulted in recent interest in its intentional production for C management, in which case it is referred to as "biochar" (Lehmann et al., 2006; Laird, 2008; Whitman et al., 2010).

As interest grows in manipulating the global C cycle to increase the soil C pool by producing biochar, it becomes important that we

better understand and, ultimately, be able to predict, its mineralization. In particular, accurately predicting the net C impact is essential for those interested in calculating C credits for biochar production and application systems (Reijnders, 2009; Whitman and Lehmann, 2009; Whitman et al., 2010). Because PyC includes diverse materials that may differ substantially from one another (Masiello, 2004; Preston and Schmidt, 2006), we aimed to progress toward a quantitative understanding of the properties that determine PyC decomposition rate. Factors known to impact mineralization of PyC include feedstock, charring temperature and charring time during PyC production, as well as the environmental conditions to which the PyC is subjected (Hilscher et al., 2009; Nguyen et al., 2010; Pereira et al., 2011). Chemical or physical changes correlated with increasing production temperature include the relative decrease in aliphatic C structures and concomitant relative increase in aromatic C structures, decreasing H/C$_{organic}$ and O/C$_{organic}$ as dehydration takes place, as well as decreasing volatile mass content (Keiluweit et al., 2010; Spokas, 2010; Singh et al., 2012b). However, these broad trends have wide variability when predicting PyC mineralization (Baldock and Smernik, 2002; Spokas, 2010; Zimmerman, 2010). Singh et al. (2012b) found C mineralization over 5 yr was strongly predicted by way of nuclear magnetic resonance (NMR)-determined proportion of nonaromatic C (exponential function, positive) and degree of aromatic condensation

* Corresponding author. Tel.: +1 607 254 1236; fax: +1 607 255 3207.
E-mail address: CL273@cornell.edu (J. Lehmann).

(power function, negative), across five feedstocks and two charring temperatures. Although an attractive possibility, it is unlikely that a single metric is the optimal way for predicting PyC stability for a broad range of materials. Studies (Kloss et al., 2012) have suggested that the chemical signature of PyC detected using Fourier transform infrared (FTIR) spectroscopy could be correlated with PyC stability, and Nguyen et al. (2008) found strong correlations of single functional groups with PyC age. It is possible that using a greater portion of the FTIR spectrum may allow stronger predictions of PyC mineralization.

In this study, transmission mode FTIR is compared to other initial properties of PyC to determine which can best predict C mineralization, using PyC with a range of feedstocks and production temperatures, and including the original feedstock materials. The vast majority of studies of PyC mineralization only examine the final product and do not account for the original feestock material or the C lost during PyC production. This may be an appropriate approach for some studies of naturally-produced PyC, but in a biochar context, where PyC is produced intentionally for C management, it is essential that the baseline scenario and the original feedstock decomposition rate be considered.

2. Material and methods

2.1. PyC preparation

PyC material was produced from six different feedstocks: corn stover (*Zea mays* L.), oak shavings (*Quercus* sp.), pine shavings (*Pinus* sp.), fryer/broiler poultry bedding consisting primarily of manure (*Gallus gallus domesticus*) mixed with sawdust, bull bedding consisting of manure (*Bos primigenius taurus*) mixed with sawdust and dairy bedding consisting of manure (*Bos primigenius taurus*) mixed with rice hulls (*Oryza sativa* L.). The feedstocks were selected to examine a range of chemical properties and to reflect typical sources of biomass that might be available for PyC production. Each feedstock was used to produce PyC at 7 different temperatures (300, 350, 400, 450, 500, 550 and 600 °C), using slow pyrolysis (DaisyReactor, BestEnergies, Inc., Cashton, WI, USA). Pre-dried (ca. 10% moisture) feedstock (ca. 3 kg) was placed in the main chamber, which was thoroughly purged with N_2 (with the mixer running). The material was heated (80–90 min) to the target temperature at a few °C/min and isothermically charred at the final temperature for ca. 15 min before the furnace was turned off and the main chamber allowed to cool. The material was collected under N_2 to reduce rapid oxidation and auto-ignition. It was stored in plastic bag-lined galvanized, epoxy-lined tin paint cans from which the ambient air was purged with a vacuum pump and replaced with Ar. Samples of the original feedstock materials were dried at 60 °C.

2.2. Sample preparation

Bottles (30 ml) were washed (10% HCl) and filled with 19.2 g white quartz sand (Sigma Aldrich no. 274739, 50 + 70 mesh; heated at 500 °C in a muffle furnace for 24 h). Each PyC sample was slightly crushed with a mortar and pestle and sieved to a particle size of 500–2000 μm. Sieved PyC (0.8 g) was hand-mixed into each sand-filled bottle. Four blank replicates of sand alone were also prepared.

Water holding capacity (WHC) was determined gravimetrically for a sample of each PyC-sand mixture using funnels and filter paper, via mass difference after saturating the mixture with distilled water and allowing it to completely drain freely.

A microbial inoculation was prepared from a soil sample from a historical charcoal blast furnace site in Cartersville, GA (Cheng et al., 2008a). The soil was noted for high PyC content and microbial activity, and we expected that the microbial community would be adapted to the presence of PyC. The sample had been stored at 4 °C after sampling, and was incubated under 60% WHC at 30 °C for 7 days. An aliquot was then mixed with distilled water to 1:50 w/v soil:water, shaken gently (30 min) and filtered through a Whatman no. 1 filter paper. The resulting solution had nutrients added to give: 4 mM NH_3NO_3, 4 mM $CaCl_2$, 2 mM KH_2PO_4, 1 mM K_2SO_4, 1 mM $MgSO_4$, 25 μM H_3BO_3, 2 μM $MnSO_4$, 2 μM $ZnSO_4$, 2 μM $FeCl_2$, 0.5 μM $CuSO_4$, and 0.5 μM Na_2MoO_4. Inoculation and micronutrient solution (1.8 ml) were added to each jar and sufficient deionized water was added to each jar to bring the mixture to 55% WHC.

2.3. Incubation analysis and C debt or credit caclulation

The bottles were incubated in a dark temperature-controlled environment at 30 °C under aerobic conditions (i.e. without caps, open to the air, with a partial cover to minimize dust deposition) in a water bath. They were maintained at 55% WHC by weighing the jars every 3 weeks and adding distilled water to bring them to the starting mass. A long-term [3 yr (1059 days), 3 replicates per PyC sample] and a short term [5 months (168 days), 4 replicates per PyC sample] incubation was prepared, where the bottles were removed after the designated length of time and samples were dried at 105 °C. Each sample was poured onto a tray. Half of each sample was reserved and half poured into ball milling jars and ground to a fine powder. The powdered samples were stored in glass vials. A subsample of each vial was weighed in a 12.5 by 5 mm Sn capsule (Elemental Microanalysis) and analyzed for total C with a NC2100 soil analyzer (ThermoQuest Italia S.p.A., Milan, Italy).

Total C lost during incubation was calculated for each PyC sample. We also calculated a C debt or credit ratio by comparing the C remaining in the incubated PyC sample with the C remaining in the incubated original feedstock material sample. A value > 1 indicates that more C remained in the PyC than in the original feedstock, while a value < 1 indicates that less C remained – i.e. C loss during PyC production outweighed the increased stability obtained through charring (Fig. 1).

2.4. Characterization of unincubated PyC

2.4.1. Proximate analysis

Volatile, ash and fixed carbon content were determined for all samples using standard methods (American Society for Testing and Materials, 2000; Enders et al., 2012). Each sample was placed
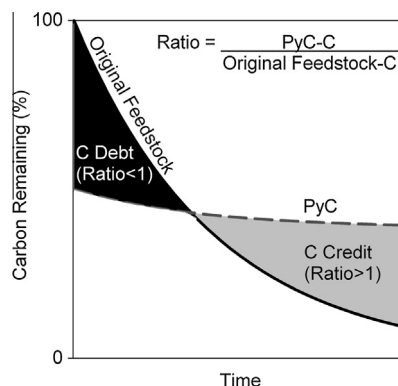

Fig. 1. Conceptual illustration of the C debt or credit ratio. Initial PyC production results in a loss of ∼50% of total C. However, remaining C in PyC decomposes more slowly than C in initial feedstock. Over time, the debt or credit ratio increases from < 1 (debt) to > 1 (credit).

in an individual desiccator upon removal from the oven to limit adsorption of water before weighing.

2.4.2. H/C and O/C

H/$C_{organic}$ and O/$C_{organic}$ ratios were determined for all samples. To measure pre-incubation C content, an aliquot (1.5–3.5 mg) of each powdered PyC sample was weighed into a 5 by 3.5 mm Sn capsule (Elemental Microanalysis), which was then sealed. Total C content was determined using a PDZ Europa ANCA-GSL elemental analyzer (PDZ Europa Ltd., Sandbach, UK). $C_{organic}$ content was determined as described by Enders et al. (2012), after addition of HCl to PyC samples to remove carbonate. For H content, an aliquot (0.4–0.6 mg) of each powdered PyC sample (ground with a mortar and pestle) was weighed into a 5 by 3.5 mm Ag capsule (Elemental Microanalysis), which was sealed. Samples were analyzed using a Hekatech HT oxygen analyzer, where samples were thermally decomposed to H_2 in a ceramic reactor filled with glassy carbon at 1345 °C (Sercon Ltd., Cheshire, UK). O content was determined as follows: $X_O = 1 - X_{Ash} - X_C - X_H$, where X_O, X_{Ash}, X_C and X_H are the fractions of O, ash, and C and H, respectively.

2.4.3. FTIR

To avoid the effect of dissociation of functional groups during the FTIR (Cheng et al., 2008b), the pH of sieved PyC samples was adjusted using pH 7 deionised water for 5 days, decanting and replacing the water twice (Nguyen and Lehmann, 2009). Samples were air dried for 2 days and dried at 60 °C. Dry PyC samples were ground (mortar and pestle) and mixed with KBr powder (dried at 105 °C) at a ratio of 3 mg PyC/1000 mg KBr for all those created < 500 °C and at a ratio of 3 mg PyC/2000 mg KBr for all PyC samples created at 500 °C and above. The adjustment was needed due to the greater absorbance of the dark and dense high temperature PyC samples and should not change results relevant to this study. The PyC-powder mixture was then re-ground (mortar and pestle) to ensure homogeneity and stored in a desiccator. Pellets were created using 150–250 mg powder in a pellet press at 30–40 J pressure. Two pellets were created for each PyC and their spectra averaged for analysis. Using a Mattson Model 5020 FTIR Spectrometer (Madison, WI) each sample was scanned 100× from 400–4000 cm^{-1}, with a resolution of 4 cm^{-1}, with subtraction of a blank value for a pure KBr pellet.

Functional groups were proportionally quantified using OMNIC 7.4 (Thermo Fisher Scientific Inc., 1992–2007). Wave numbers were assigned according to Dutta et al. (2007), Pandey and Pitman (2003), Politou et al. (1990) and Lehmann and Solomon (2010): 3425 cm^{-1} to O—H stretch in carboxylic acids, phenols and alcohols as well as N—H stretch, 2925–2870 cm^{-1} to aliphatic C—H stretch of CH_3 and CH_2, 1700 cm^{-1} to C=O stretch, 1590 cm^{-1} to aromatic C=C vibrations and stretching, 1424 cm^{-1} and 1460 cm^{-1} to C—H deformation in lignin and carbohydrates, 1374 cm^{-1} to aliphatic deformation of CH_2 or CH_3 groups in cellulose and hemicellulose, 1048 cm^{-1} to C—O stretching in cellulose and hemicellulose, and 816 cm^{-1} to aromatic C—H out of plane deformation. These wavenumbers were chosen because they represent functional groups that were clearly identifiable in most spectra. Relative proportions of selected species were calculated from signal height after drawing a baseline for each signal position, baseline correction and spectrum normalization. This "fractional signal height" was calculated by dividing the signal height for each species by the summed signal heights of all species of interest, thus giving a measure of its relative contribution to the spectra relative to the other species of interest.

Baselines drawn were: 3691–3118 for O—H stretch, 3006–2803 for aliphatic CH stretch, 1667–1745 for C=O stretch, 1509–1666 for C=C vibrations and stretch, 1483–1466 for C—H deformation in lignin and carbohydrates, 1400–1330 for C—H deformation in

cellulose/hemicellulose, 1145–910 for C—O stretching in cellulose and hemicellulose and 895–743 for aromatic C—H deformation.

2.5. Data analysis

Similarities between full FTIR spectra of all PyC and original feedstock samples were visualized by constructing a dendrogram using Ward's hierarchical clustering method (JMP Pro 9 statistical program). During hierarchical clustering, the two most similar spectra are grouped in a single cluster, which is then repeated step by step, combining similar clusters until all spectra are ordered hierarchically in a "tree" based on similarity.

Full FTIR spectra were used to predict 3 yr C loss across PyC samples using partial least squares regression (PLSR). PLSR is a linear regression of one or more responses (here, mean C loss), onto a set of principal component scores derived from a predictor matrix (here, FTIR spectral data), where the covariance between the response and scores are maximized. The strength of the correlation was cross-validated using the "leave-one-out" approach, where each sample was consecutively withheld while re-running the PLSR and then tested for congruence with the resulting regression, resulting in a set of predicted and measured values for which an R^2 value was calculated. The data were analyzed using the pls package (Mevik and Wehrens, 2007) in the statistical computing language and environment R (R Development Core Team, 2010).

ANOVA was used to analyze C loss data for PyC materials with temperature (categorical) and feedstock as predictor variables. A series of linear regressions was performed, correlating C loss data with initial parameters, and a multiple regression was performed using the fractional signal heights for all FTIR wavenumbers as factors (except 3691–3118, which was not assigned to a C bond type). A multiple linear regression was also performed, correlating C debt or credit ratio with the fractional signals at 1590, 1374, 2925, and 1460 cm^{-1} for the PyC materials, and the corresponding fractional signals of the original feedstock materials at 2925 and 1700 cm^{-1}. The analyses were performed using JMP 9 statistical software (JMP, Version 9. SAS Institute Inc., Cary, NC, 1989–2009).

3. Results

3.1. PyC characteristics and FTIR functional group chemistry

Increasing production temperature had a similar effect on FTIR spectra from different feedstocks, with the exception of poultry manure with sawdust (Figs. 2 and 3; Supporting Figs. S1–S5) (spectra from pine feedstock and corresponding PyC are shown as an example in Fig. 2; all other spectra in Supporting information) This is clearly shown in the dendrogram (Fig. 3), where the poultry PyC materials tend to cluster together, while the other PyC materials cluster by temperature. The FTIR scans of the poultry manure mixed with sawdust were dominated by a strong signal likely from $CaCO_3$ (Supporting Fig. S1), which obscured signals of interest, particularly in the fingerprint region of the spectrum, where many bond signatures co-occurred. This is consistent with analysis of the same set of PyC materials reported in the Supplementary information of Enders et al. (2012), which showed that there were substantial quantities of inorganic C in the PyC materials from poultry manure with sawdust, but not in PyC from any of the other feedstocks investigated here. Briefly, as charring temperature increased, the proportion of 1590 cm^{-1} C=C and 816 cm^{-1} aromatic C—H groups increased, while the proportions of 1700 cm^{-1} C=O, 2925–2870 cm^{-1} CH_2 and CH_3, 3400 cm^{-1} O—H, 1375 cm^{-1} CH_2 and CH_3, 1425 cm^{-1} lignin and carbohydrate C—H, and 1048 cm^{-1} cellulose and hemicellulose C—O groups decreased (Supporting Table S1). Correlations between other initial
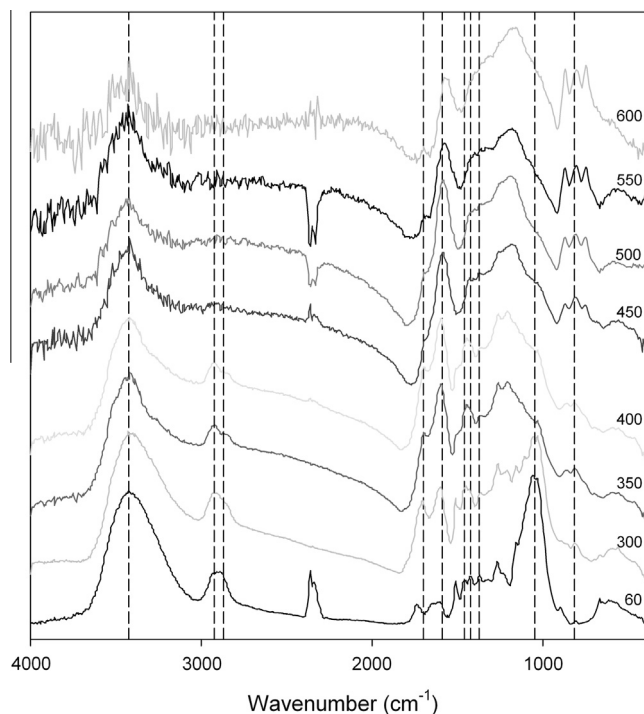
Fig. 2. Representative set of FTIR spectra for pine feedstock vs. temperatures (spectra for other PyC materials are in Supporting information). Vertical lines indicate the location of signals assigned to functional groups, as described in the text (3425 cm^{-1}, O–H stretch in carboxylic acids, phenols and alcohols, as well as N–H stretch; 2925–2870 cm^{-1}, aliphatic C–H stretch of CH$_3$ and CH$_2$; 1700 cm^{-1}, C=O stretch; 1590 cm^{-1}, aromatic C=C vibrations and stretching; 1424 cm^{-1} and 1460 cm^{-1}, C–H deformation in lignin and carbohydrates; 1374 cm^{-1}, aliphatic deformation of CH$_2$ or CH$_3$ groups in cellulose and hemicellulose; 1048 cm^{-1}, C–O stretching in cellulose and hemicellulose; 816 cm^{-1}, aromatic C–H out of plane deformation).

PyC properties and FTIR results are described in Supporting Table S2.

Chemical properties of PyC (C/N, H/C, O/C and pH) are reported in Supporting Table S3. Briefly, C/N values were very high (300–850) for the PyC from wood, mid-range (30–80) for PyC from bull manure with sawdust, dairy manure with rice hulls, and corn stover, and low for the poultry PyC (10–22). H/C$_{organic}$ and O/C$_{organic}$ values tended to decrease with increasing charring temperature, and were relatively similar for PyC from the various feedstocks, with the exception of PyC from poultry manure with sawdust, which had higher O/C$_{organic}$ values and lower H/C$_{organic}$ values. PyC from bull manure with sawdust, dairy manure with rice hulls, poultry manure with sawdust, and corn stalks had pH values ranging from around 8–10, while the two wood PyCs had lower pH values ranging from around 4.5–8. The pH of the PyC tended to increase with increasing production temperature for most feedstocks.

Proximate analysis data are listed in Supporting Table S4 and are reported and discussed in greater detail by Enders et al. (2012). Briefly, for most PyC, volatile matter was highest at the two lowest temperatures. The exception was the PyC from poultry manure, which showed little trend in the volatile matter with increasing charring temperature. Ash content exhibited a less striking trend, increasing only slightly at higher temperature. Again, PyC from poultry manure with sawdust was the exception, with very high ash content (ca. 50%).

3.2. PyC mineralization

C losses were greatest for the original feedstocks, with significant C loss for all original feedstocks at 5 months and 3 yr (Fig. 4;
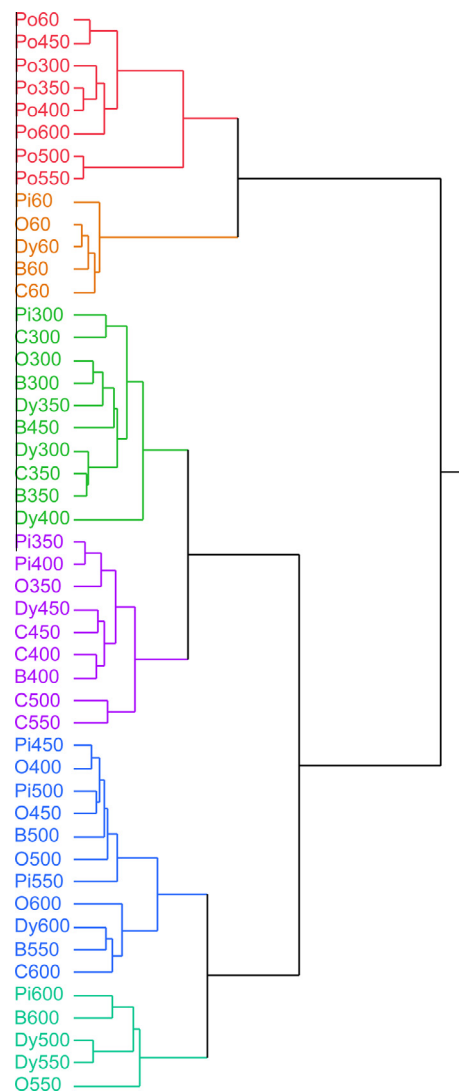

Fig. 3. Dendrogram showing FTIR spectra similarity based on Ward's hierarchical clustering method. B, bull manure with sawdust; C, corn stover; Dy, dairy manure with rice hulls; O, oak; Pi, pine; and Po, poultry manure with sawdust (numbers represent charring or drying temperature).

Supporting Tables S5 and S6). After 3 yr, 300 °C PyC materials lost significantly more C than higher temperature PyC materials (LSMeans contrast, $p = 0.0003$), but significant differences in C loss between PyC materials produced at temperatures $\geqslant 350$ °C were not detectable with our method (Tukey's HSD, $p > 0.05$). There was no significant feedstock effect on mineralization, except for poultry manure with sawdust material, which had significantly greater C loss than all other materials (Tukey's HSD, $p < 0.05$).

PyC production resulted in a substantial initial C loss from the unpyrolysed feedstock (C debt), as shown by the black portion of the bars in Fig. 5. However, the relatively lower subsequent C loss in PyC during decomposition as compared with the initial feedstock could eventually result in a net C retention (C credit), as indicated by the hashed bars in Fig. 5. Over 3 yr, the C debt or credit ratio for all bull, corn, dairy and poultry PyC samples increased, reaching values significantly above unity (resulting in net C credit) for all corn PyC samples and some bull, dairy and poultry PyC samples (Fig. 5). However, no woody PyC samples reached unity after 3 yr of incubation (thus remaining in net C debt).
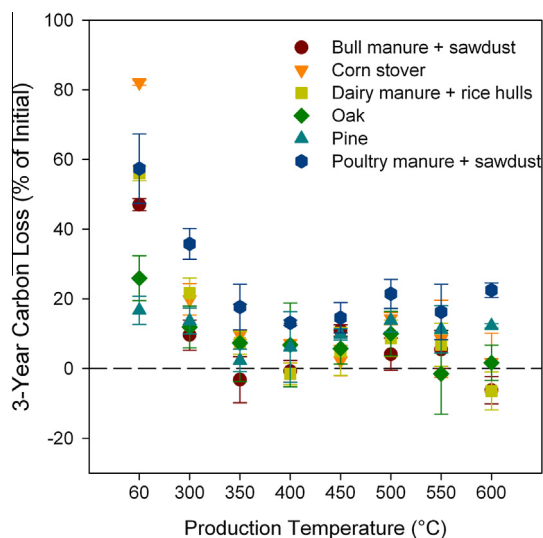
Fig. 4. Carbon loss after 3 years of incubation, for each PyC feedstock and temperature, including original material dried at 60 °C. Error bars represent 1 SE ($n = 3$).
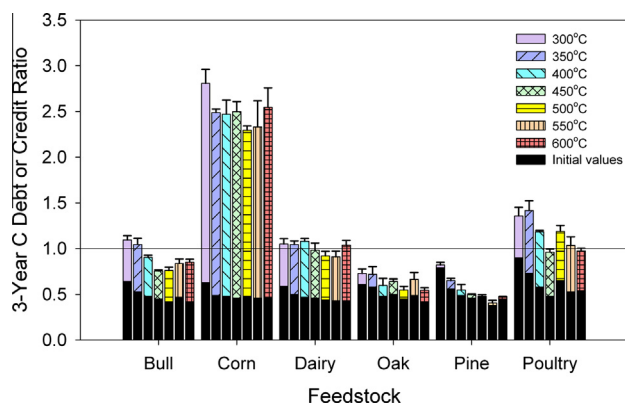
Fig. 5. Carbon debt or credit ratio after 3 years of incubation. Black bars indicate initial values (directly after PyC production), while shaded and patterned bars indicate status after 3 years. Error bars represent 1 SE ($n = 3$). Horizontal line indicates the "break-even" point above which there is net C stabilization, or credit, and below which a C debt remains.

3.3. Correlation of chemical properties and mineralization

Linear relationships with 3 yr C loss were not very strong, with the FTIR parameters and the $H/C_{organic}$ and $O/C_{organic}$ ratios providing the best correlations, while proximate analysis data were less effective as predictors of C loss (Supporting Table S7). Better correlations using a single parameter could be obtained using a log fit for the fractional FTIR signals at 1590 (associated with C=C bonds) (R^2 0.67) and 816 cm^{-1} (associated with aromatic C—H bonds) (R^2 0.47) (Supporting Fig. S6), or an exponential fit for $H/C_{organic}$ (R^2 0.65) and $O/C_{organic}$ (R^2 0.60) (Fig. 6).

We improved predictive ability substantially by fitting a multiple linear regression using the fractional FTIR signals at 816, 1048, 1374, 1424, 1460, 1590, 1700 and 2925 cm^{-1} as parameters to predict mean C remaining for all PyC and original materials (R^2 0.80, $p < 0.0001$) and for PyC only (R^2 0.45, $p < 0.03$) (Table 1). When using PLSR to capture the information in the full FTIR spectrum, however, we found a relatively weak cross validation R^2 value of 0.33.

The C debt or credit ratio was also predictable using fractional FTIR signals. The multiple linear regression model with the

fractional signals at 1590, 1374, 2925 and 1460 cm^{-1}, plus the corresponding fractional signals of the original feedstock materials at 2925 and 1700 cm^{-1}, as factors, provided a good fit (R^2 0.90, $p < 0.0001$).

4. Discussion

4.1. C loss and the C debt or credit ratio

Total C loss after the 3 yr incubation was within the range observed in other PyC incubation experiments of similar duration using direct (Kuzyakov et al., 2009; Zimmerman, 2010; Bruun et al., 2012) and indirect (Nguyen and Lehmann, 2009) measurements of CO_2 evolution. This study's indirect method was unable to allow detection of small differences in C loss between PyC samples produced at $\geqslant$ 350 °C, while similar studies noted a significant decrease in loss at higher production temperatures (Zimmerman, 2010; Singh et al., 2012b), likely due to greater precision with direct measurements. While direct methods offer improvements in precision, they still may not be sufficient for differentiating long-term stability differences in higher temperature PyC samples unless they are conducted over multiple years to allow extrapolation of the decreasing mineralization rate (Zimmerman, 2010).

One approach for characterizing PyC mineralization is to divide it into "labile" and "recalcitrant" pools (Roberts et al., 2010; Whitman et al., 2011; Singh et al., 2012a). The approach is useful conceptually and for modeling, but separating these pools quantitatively is a matter of methodological definition (Cross and Sohi, 2011, 2012). As higher incubation temperatures and longer incubation times are chosen to determine "labile C", this pool will be calculated to be larger, while the half life of the remaining "recalcitrant" pool will be calculated to be longer (Singh et al., 2012a). In this study, significant C loss still occurred for PyC samples after 5 months so, in order to conservatively assess the minimum "recalcitrant fraction" for a given PyC – i.e. a fraction that would have a half life of hundreds to thousands of years, incubation studies > 1 yr under optimum conditions for mineralization, as implemented in this study, are likely to be necessary.

While C loss was not different between PyC samples produced at $\geqslant$ 350 °C, C loss differed significantly between the incubated original feedstock materials. The relative mineralization rate of the original materials was largely determined from their chemical composition. For example, corn stover tended to be dominated by relatively easily-"mineralizable" compounds, such as cellulose and hemicellulose (indicated by the aliphatic deformation of CH_2 or CH_3 groups at 1374 cm^{-1}), while woody feedstocks have higher lignin content, and mineralize more slowly (Melillo et al., 1982; Zhang et al., 2008). This makes feedstock a key determinant of the C debt or credit ratio. The PyC samples that were able to compensate for the initial C debt of PyC production after 3 yr were those for which the original feedstock lost the most C from mineralization. Most notable were corn stover PyC samples, which reached C debt or credit ratios of 2.3–2.8, and the other non-woody feedstocks, many of which reached the "break even point" of 1.0 after 3 yr. However, for PyC samples with slow-decaying original feedstock material, such as pine and oak, the C loss incurred immediately through PyC production left the PyC with a C debt that was not readily compensated for by the greater stability of PyC. While increasing the PyC production temperature > 350 °C likely increases the stability of its remaining C over the long term (Singh et al., 2012b), this effect was not detectable over the timescale of this study and with the sensitivity of these methods. Furthermore, these higher production temperatures resulted in greater initial C losses at the time of PyC production. Thus, depending on the feedstock and the timeline of interest, producing a relatively low tem-
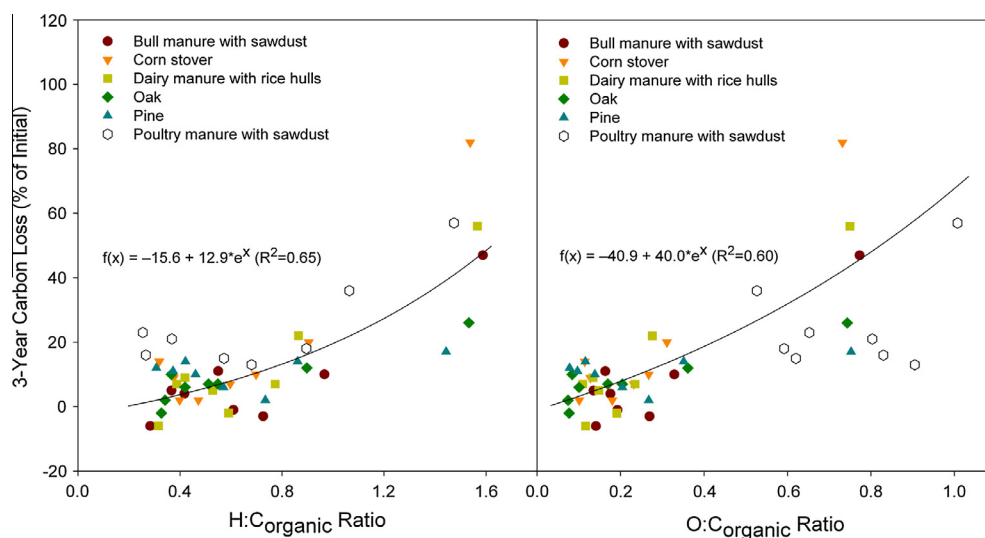
Fig. 6. Left: H:C$_{organic}$ vs C loss. Right: O:C$_{organic}$ vs. C loss for all PyC (grouped by original materials) and their corresponding original material samples. Fit lines were calculated excluding poultry data (open circles).

Table 1
Coefficients for multiple linear regression of mean C remaining ± standard error for each included fractional signal height of all major FTIR wavenumbers (cm^{-1}) (excluding poultry bedding samples).

Parameter	PyC and feedstocks (R^2 = 0.80)	PyC only (R^2 = 0.45)
Intercept	101 ± 16	78 ± 12
816 cm^{-1}	−19 ± 22	29 ± 19
1048 cm^{-1}	−197 ± 86	−131 ± 74
1374 cm^{-1}	−151 ± 34	297 ± 124
1424 cm^{-1}	140 ± 259	200 ± 124
1460 cm^{-1}	64 ± 169	116 ± 126
1590 cm^{-1}	12 ± 31	25 ± 22
1700 cm^{-1}	−43 ± 66	−57 ± 54
2925 cm^{-1}	−41 ± 70	15 ± 50

perature PyC (e.g. 350 °C) may result in greater C savings than producing a higher temperature PyC (e.g. 600 °C), even though the C that remains in the 600 °C PyC may be more stable.

These findings have important implications for the use of biochar as a C management tool. The C debt or credit ratio will continue to change as long as the fresh material and the PyC continue to decay at different rates, so the ratio and its rate of change could provide a metric for the relative stability of the two materials over time. However, this metric must be understood in the context of the baseline conditions for each system. For example, if the fresh feedstock were left to decay in a warm, moist field, we would expect that decay would be faster than measured here, increasing the C debt or credit ratio, whereas if the feedstock were dried and kept in cool dry conditions, we would expect the biochar to take longer to "break even". Thus, the specific conditions of each system should be taken into account when applying this ratio, including climatic variables and interactions with minerals (Brodowski, 2004) or existing soil OM (Kimetu and Lehmann, 2010; Jones et al., 2011; Luo et al., 2011). This study indicates that PyC production for C stabilization will have the greatest C benefit for feedstocks that would be mineralized rapidly, while less easily "mineralizable" feedstocks, such as woody feedstocks, would take longer to accrue a C stabilization benefit, and might result in a C debt for many years after PyC production (Supporting Fig. S7).

Our C debt or credit ratio is a step toward evaluating the full C impact of PyC production on the C balance. However, the net C impact of a PyC system will extend beyond the stability of the PyC and its feedstock, to include the energy required for its production,

any energy captured during its production and the impact of PyC on growing biomass and soil C stocks, among many other factors (Gaunt and Cowie, 2009). For example, greater energy may be required to produce the higher temperature PyC materials, which could further move the C balance toward a C debt status. Additionally, PyC addition to soils has been found to both stimulate and reduce soil OM decomposition (Keith et al., 2011; Zimmerman et al., 2011), increasing or decreasing the net C impact of PyC at a system level. These effects depend on the particular PyC, its production conditions, engineering solutions, soil type, environmental conditions and timescale, and would need to be accounted for in order to correctly determine the net C impact of an entire PyC system, although the scope of this goes beyond this study.

4.2. Prediction of PyC mineralization from initial properties

It would be ideal to be able to predict C loss using measurable quantities that did not depend on a priori knowledge of the PyC production conditions or feedstock. The initial PyC properties have differing degrees of success at predicting the C loss using simple linear correlations. Elemental ratios and FTIR data often outperform proximate analysis data, for which correlations are largely driven by the poultry PyC and original materials. Applying more sensitive measurement techniques for PyC loss may not improve correlation with proximate analysis, as Zimmerman's (2010) 1 yr-study, using direct measurements of CO$_2$ loss, and Cross and Sohi's (2012) chemical oxidation method yielded similar correlation coefficients (0.35 and 0.53, respectively). Exponential fits with the O/C$_{organic}$ and H/C$_{organic}$ ratios provided good prediction of C loss, when low temperature PyC samples and original materials were included [supporting the proposal by Spokas (2010) for O/C as a predictor] but, in our study, did not distinguish well between PyC samples with the lowest extent of mineralization when excluding materials with high H/C$_{organic}$ (> 0.80) and O/C$_{organic}$ (> 0.27), likely due to the low sensitivity of our method for detecting C loss at very low mineralization. Additionally, elemental ratios are likely most appropriate for comparing PyC samples with similar ash content, e.g. < 20% (Enders et al., 2012). FTIR spectral information allowed us to easily differentiate PyC materials from each other, confirming earlier studies (Politou et al., 1990; Keiluweit et al., 2010; Chatterjee et al., 2012). Log transforming these FTIR data (Supporting Fig. S6) and fitting exponential models to the ele-

mental ratio data (Fig. 6) further improved their predictive ability. However, none of these models matched the quality of fit achieved by Singh et al. (2012b), using 5 yr incubation data and nonaromatic C or degree of aromatic condensation as determined from ^{13}C CP NMR (R^2 0.91 and 0.86, respectively). While our simple correlations are useful for identifying candidate predictor variables, the FTIR spectra are data-rich, potentially providing greater predictive power when more information contained in the spectrum is used, unlike an elemental ratio or proximate analysis parameter, which are limited to a single value.

However, using the entire FTIR spectrum in the PLSR analysis was not very successful for predicting C loss for the present data set. This is likely due to the still relatively low number of samples available for PLSR analysis and the difficulty in detecting differences in C remaining across the higher temperature PyC samples with our C loss method. In contrast, the strong correlation (R^2 0.80) achieved using multiple linear regression of the fractional signal height of FTIR functional groups indicates that using a suite of select signals from FTIR data could be a robust and inexpensive way of predicting C loss from PyC samples. Additionally, it may indicate that complex changes during charring beyond simply deoxygenation and dehydration (Keiluweit et al., 2010) are important in predicting C loss from PyC. Still, it is important to note that FTIR as applied here is not quantitative – i.e. if the proportion of one kind of bond were to double for a PyC upon heating, its associated signal height might not double. Thus, more data are needed to establish predictions of C loss using the full spectral information by way of PLSR analysis and calibration of the relationship between any FTIR data and PyC loss would likely be necessary if applied to PyC types that were not in the original data set. This is commensurate with the use of IR data for prediction of PyC in soils (Janik et al., 2007).

5. Conclusions

The C debt or credit ratio is an essential tool for assessing the C impact of PyC production and application for C management. Our findings highlight the idea that, regardless of the mineralization of the PyC produced, if its original feedstock decomposes slowly, PyC production would not likely result in C savings for many years. To determine the net C impact of a PyC system, the C debt or credit ratio may be combined with a systems-level accounting of all greenhouse gas costs and benefits, including energy and impact on non-PyC soil C.

While elemental ratios provided an improvement over proximate analysis for predicting short term C loss in this study, predicting C loss from the initial characteristics of PyC was most successful using a multi-signal, multivariate linear regression model with FTIR data. However, such approaches still require calibration. Using a larger dataset of FTIR spectra and direct C loss measurements might improve PLSR-based predictive models. Future research should aim to refine methods for predicting the fraction of easily-"mineralizable" PyC from its initial properties and to investigate new methods that could accurately assess long term mineralization of the less readily mineralizable fraction of PyC.

Acknowledgements

Appendix A. Supplementary material

Supplementary data associated with this article can be found, in the online version, at http://dx.doi.org/10.1016/j.orggeochem. 2013.09.006.

Associate Editor – **S. Derenne**

References

American Society for Testing and Materials, 2000. Standard Test Method for Chemical Analysis of Wood Charcoal. Standard D1762-84(2001). Annual book of ASTM standards. Section 4: Construction. Volume 04.10: Wood, pp. 293–294.

Baldock, J.A., Smernik, R.J., 2002. Chemical composition and bioavailability of thermally, altered *Pinus resinosa* (Red Pine) wood. Organic Geochemistry 33, 1093–1109.

Bird, M.I., Ascough, P.L., 2012. Isotopes in pyrogenic carbon: a review. Organic Geochemistry 42, 1529–1639.

Brodowski, S.B., 2004. Origin, Function, and Reactivity of Black Carbon in the Arable Soil Environment. PhD Thesis, University of Bayreuth, Bayreuth, Germany.

Bruun, E.W., Ambus, P., Egsgaard, H., Hauggaard-Nielsen, H., 2012. Effects of slow and fast pyrolysis biochar on soil C and N turnover dynamics. Soil Biology and Biochemistry 46, 73–79.

Chatterjee, S., Santos, F., Abiven, S., Itin, B., Stark, R.E., Bird, J.A., 2012. Elucidating the chemical structure of pyrogenic organic matter by combining magnetic resonance, mid-infrared spectroscopy and mass spectrometry. Organic Geochemistry 51, 35–44.

Cheng, C.H., Lehmann, J., Thies, J.E., Burton, S.D., 2008a. Stability of black carbon in soils across a climatic gradient. Journal of Geophysical Research-Biogeosciences 113, G2.

Cheng, C.H., Lehmann, J., Engelhard, M., 2008b. Natural oxidation of black carbon in soils: changes in molecular form and surface charge along a climosequence. Geochimica et Cosmochimica Acta 72, 1598–1610.

Cross, A., Sohi, S.P., 2011. The priming potential of biochar products in relation to labile carbon contents and soil organic matter status. Soil Biology and Biochemistry 43, 2127–2134.

Cross, A., Sohi, S.P., 2012. A method for screening the relative long-term stability of biochar. Global Change Biology Bioenergy. http://dx.doi.org/10.1111/gcbb.12035.

Dutta, S., Brocke, R., Hartkopf-Froder, C., Littke, R., Wilkes, H., Mann, U., 2007. Highly aromatic character of biogeomacromolecules in Chitinozoa: a spectroscopic and pyrolytic study. Organic Geochemistry 38, 1625–1642.

Enders, A., Hanley, K., Whitman, T., Joseph, S., Lehmann, J., 2012. Characterization of biochars to evaluate recalcitrance and agronomic performance. Bioresource Technology 114, 644–653.

Gaunt, J., Cowie, A., 2009. Biochar, greenhouse gas accounting and emissions trading. In: Lehmann, J., Joseph, S. (Eds.), Biochar for Environmental Management: Science and Technology. Earthscan, London, pp. 317–340.

Hilscher, A., Heister, K., Siewert, C., Knicker, H., 2009. Mineralisation and structural changes during the initial phase of microbial degradation of pyrogenic plant residues in soil. Organic Geochemistry 40, 332–342.

Janik, L.J., Skjemstad, J.O., Shepherd, K.D., Spouncer, L.R., 2007. The prediction of soil carbon fractions using mid-infrared-partial least square analysis. Australian Journal of Soil Research 45, 73–81.

Jones, D.L., Murphy, D.V., Khalid, M., Ahmad, W., Edwards-Jones, G., DeLuca, T.H., 2011. Short-term biochar-induced increase in soil CO$_2$ release is both biotically and abiotically mediated. Soil Biology and Biochemistry 43, 1723–1731.

Keiluweit, M., Nico, P.S., Johnson, M.G., Kleber, M., 2010. Dynamic molecular structure of plant biomass-derived black carbon (biochar). Environmental Science & Technology 44, 1247–1253.

Keith, A., Singh, B., Singh, B.P., 2011. Interactive priming of biochar and labile organic matter mineralization in a smectite-rich soil. Environmental Science and Technology 45, 9611–9618.

Kimetu, J.M., Lehmann, J., 2010. Stability and stabilisation of biochar and green manure in soil with different organic carbon contents. Australian Journal of Soil Research 48, 577–585.

Kloss, S., Zehetner, F., Dellantonio, A., Hamid, R., Ottner, F., Liedtke, V., Schwanninger, M., Gerzabek, M.H., Soja, G., 2012. Characterization of slow pyrolysis biochars: effects of feedstocks and pyrolysis temperature on biochar properties. Journal of Environmental Quality 41, 990–1000.

Krull, E., Lehmann, J., Skjemstad, J., Baldock, J., Spouncer, L., 2008. The global extent of black C in soils: is it everywhere? In: Schröder, H.G. (Ed.), Grasslands: Ecology, Management and Restoration. Nova Science Publishers, Inc., Hauppage, NY, pp. 13–17.

Kuzyakov, Y., Subbotina, I., Chen, H.Q., Bogomolova, I., Xu, X.L., 2009. Black carbon decomposition and incorporation into soil microbial biomass estimated by C-14 labeling. Soil Biology and Biochemistry 41, 210–219.

Laird, D.A., 2008. The charcoal vision: a win–win–win scenario for simultaneously producing bioenergy, permanently sequestering carbon, while improving soil and water quality. Agronomy Journal 100, 178–181.

Lehmann, J., Solomon, D., 2010. Organic carbon chemistry in soils observed by synchrotron-based spectroscopy. In: Singh, B., Gräfe, M. (Eds.), Synchroton-based Techniques in Soils and Sediment. Elsevier, Amsterdam, pp. 289–312.

Lehmann, J., Gaunt, J., Rondon, M., 2006. Bio-char sequestration in terrestrial ecosystems – a review. Mitigation and Adaptation Strategies for Global Change 11, 403–427.

Luo, Y., Durenkamp, M., De Nobili, M., Lin, Q., Brookes, P.C., 2011. Short term soil priming effects and the mineralisation of biochar following its incorporation to soils of different pH. Soil Biology and Biochemistry 43, 2304–2314.

Masiello, C.A., 2004. New directions in black carbon organic geochemistry. Marine Chemistry 92, 201–213.

Melillo, J.M., Aber, J.D., Muratore, J.F., 1982. Nitrogen and lignin control of hardwood leaf litter decomposition dynamics. Ecology 63, 621–626.

Mevik, B.-H., Wehrens, R., 2007. The pls package: principle component and partial least squares regression in R. Journal of Statistical Software 18, 1–24.

Nguyen, B.T., Lehmann, J., 2009. Black carbon decomposition under varying water regimes. Organic Geochemistry 40, 846–853.

Nguyen, B.T., Lehmann, J., Kinyangi, J., Smernik, R., Riha, S.J., Engelhard, M., 2008. Long-term black carbon dynamics in cultivated soil. Biogeochemistry 89, 295–308.

Nguyen, B.T., Lehmann, J., Hockaday, W.C., Joseph, S., Masiello, C.A., 2010. Temperature sensitivity of black carbon decomposition and oxidation. Environmental Science and Technology 44, 3324–3331.

Ohlson, M., Dahlberg, B., Økland, T., Brown, K.J., Halvorsen, R., 2009. The charcoal carbon pool in boreal forest soils. Nature Geoscience 2, 692–695.

Pandey, K.K., Pitman, A.J., 2003. FTIR studies of the changes in wood chemistry following decay by brown-rot and white-rot fungi. International Biodeterioration & Biodegradation 52, 151–160.

Pereira, R.C., Kaal, J., Arbestain, M.C., Lorenzo, R.P., Aitkenhead, W., Kedley, M., Macías, F., Hindmarsh, J., Macía-Agulló, J.A., 2011. Contribution to characterisation of biochar to estimate the labile fraction of carbon. Organic Geochemistry 42, 1331–1342.

Politou, A.S., Morterra, C., Low, M.J.D., 1990. Infrared studies of carbons. 12. The formation of chars from a polycarbonate. Carbon 28, 529–538.

Preston, C.M., Schmidt, M.W.I., 2006. Black (pyrogenic) carbon: a synthesis of current knowledge and uncertainties with special consideration of boreal regions. Biogeosciences 3, 397–420.

Reijnders, L., 2009. Are forestation, bio-char and landfilled biomass adequate offsets for the climate impacts of burning fossil fuels? Energy Policy 37, 2839–2841.

Roberts, K.G., Gloy, B.A., Joseph, S., Scott, N.R., Lehmann, J., 2010. Life cycle assessment of biochar systems: estimating the energetic, economic, and climate change potential. Environmental Science and Technology 44, 827–833.

Singh, N., Abiven, S., Torn, M.S., Schmidt, M.W.I., 2012a. Fire-derived organic carbon in soil turns over on a centennial scale. Biogeosciences 9, 2847–2857.

Singh, B.P., Cowie, A.L., Smernik, R.J., 2012b. Biochar carbon stability in a clayey soil as a function of feedstock and pyrolysis temperature. Environmental Science & Technology 46, 11770–11778.

Spokas, K.A., 2010. Review of the stability of biochar in soils: predictability of O:C molar ratios. Carbon Management 1, 289–303.

Whitman, T., Lehmann, J., 2009. Biochar – one way forward for soil carbon in offset mechanisms in Africa? Environmental Science and Policy 12, 1024–1027.

Whitman, T., Scholz, S., Lehmann, J., 2010. Biochar projects for mitigating climate change: an investigation of critical methodology issues for carbon accounting. Carbon Management 1, 89–107.

Whitman, T., Nicholson, C.F., Torres, D., Lehmann, J., 2011. Climate change impact of biochar cook stoves in western Kenyan farm households: system dynamics model analysis. Environmental Science & Technology 45, 3687–3694.

Zhang, D., Hui, D., Luo, Y., Zhou, G., 2008. Rates of litter decomposition in terrestrial ecosystems: global patterns and controlling factors. Journal of Plant Ecology 1, 85–93.

Zimmerman, A.R., 2010. Abiotic and microbial oxidation of laboratory-produced black carbon (biochar). Environmental Science & Technology 44, 1295–1301.

Zimmerman, A.R., Gao, B., Ahn, M.-Y., 2011. Positive and negative carbon mineralization priming effects among a variety of biochar-amended soils. Soil Biology and Biochemistry 43, 1169–1179.